J|A|C|S
COMMUNICATIONS

Published on Web 12/08/2008

A "Kite" Shaped Styryl End-Capped Benzo[2,1-*b*:3,4-*b*′]dithiophene with High Electrical Performances in Organic Thin Film Transistors

Yahia Didane,[†] Georg H. Mehl,[‡] Atsufumi Kumagai,[§] Noriyuki Yoshimoto,[§] Christine Videlot-Ackermann,*[,†] and Hugues Brisset*[,†]

Ingénierie Moléculaire et Matériaux Fonctionnels, Centre Interdisciplinaire de Nanoscience de Marseille (CINaM), CNRS UPR 3118, Campus Luminy, Aix Marseille Université, Marseille, France, Department of Chemistry, University of Hull, Hull, U.K., and Graduate School of Engineering, Iwate University, Morioka, Japan

Received September 29, 2008; E-mail: videlot@cinam.univ-mrs.fr; brisset@univmed.fr

It is the generally held view that high electronic performances of organic thin film transistors (OTFTs) requires strong π-orbital overlap between adjacent organic molecules in the solid state, and thus molecular design has focused on large planar systems.[1] In this context linear unsubstituted acenes receive particular attention due to their natural planarity induced by the fused benzene rings.[2] However substantial deformations from planarity can be induced simply by the attachment of bulky substituents to such molecules which eliminate significant aryl−aryl close contacts in the crystalline phase, making them excellent candidates for organic light emitting diodes (OLEDs).[2] In this case the end-to-end twist characterizes the torsion angle made by phenyl rings at both extremities of the molecule. Characteristic for such twistacenes is that the whole conjugated system is a helical distortion to the long axis of the molecule.[3] In the α-oligothiophene family the twist deformation is due at first to free rotation bound to the presence of σ-bonds between each ring and possibly stressed by substituents grafted on the conjugated backbone. Fused oligothiophenes and thiophene-acene oligomers are very attractive for maximizing the π-orbital overlap by a reduction of the freedom of rotation in the oligomer and possibly inducing a densely packed crystal structure toward face-to-face π-stacking motifs.[4] Consequently coplanar arrangement and face-to-face stacking rather than herringbone arrangements in which edge-to-face interactions dominate are expected to increase mobilities in OTFTs.[5]

Based on these considerations we decided to undertake the synthesis and investigation of a simply bridged derivative of distyryl-bithiophene (**DS2T**) for which we obtained very good electrical performances ($\mu = 0.02$ cm^2/V•s, $I_{on}/I_{off} \approx 10^5$, $S > 15$ V/decade).[6] Contrary to our expectation, the new unsubstituted distyryl-bisthienobenzene **1** obtained is not planar and the observed deformation is, to our knowledge, new to the thiophene-acene oligomer family. For the fused core we do not observe a twist deformation as in acenes but a curvature such as in bowl shaped systems.[7] As the semiconductor **1** is linear the naming "kite" twist seems to be a more appropriate description. Initially perceived to be undesirable, **1**-based OTFTs exhibit rather surprisingly, in contrast to the generally held view, excellent performance in air ($\mu = 0.1$ cm^2/V.s, $I_{on}/I_{off} > 10^6$; $S < 4$ V/decade) higher by a factor of 5 than the parent unbridged coplanar semiconductor **DS2T**.

The synthesis of **1** is shown schematically in Scheme 1. Dilithiation of 3,3′-diformylacetal-2,2′-bithiophene **5** using *n*-BuLi at −78 °C followed by the addition of DMF gave **4**. The Wittig−Horner olefination between **4** and benzylphosphonate lead to the diacetal **3**. Hydrolysis of acetal groups with acetic acid gave

Scheme 1. Synthesis Pathway of **1** (Full Synthetic Details for **4**, **3**, **2**, and **1** Are Provided in the Supporting Information)

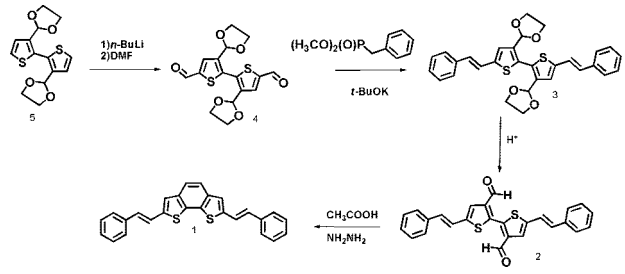

the dialdehyde-distyryl-bithiophene **2** as a stable yellow solid. Treatment of **2** with hydrazine resulted in the styryl end-capped benzo[2,1-*b*:3,4-*b*′]dithiophene **1**.

Single crystals of **1** were grown by slow evaporation of a saturated methylene chloride solution, and the crystal structure was determined by X-ray diffraction.[8] Figure 1a and 1b show the molecular shape of **1** and a packing view of the **1** crystal, respectively. It demonstrates that the fused core and moreover the extended π-conjugated system are not planar.

The molecular shape and crystal organization differ significantly from those of the unbridged analogue which is linear and coplanar (Supporting Information, Figures S1−S3). Perepichka et al. reported a fully planar geometry for tetrathienoanthracene with an intramolecular distance between sulfur atoms of 3.533 Å, lower than the sum of van der Waals radii.[9] For **1** the intramolecular distance

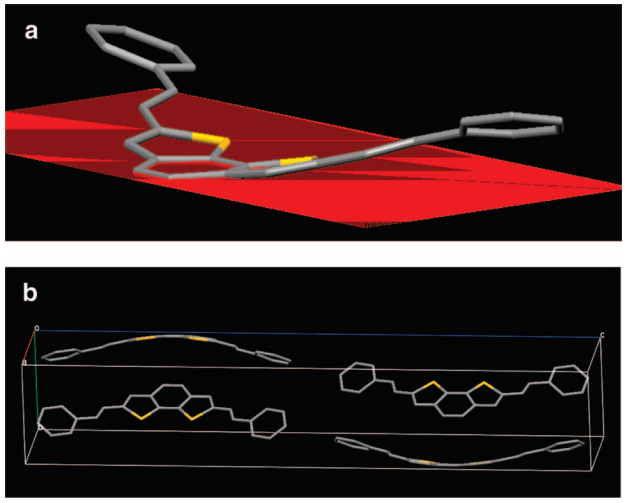

Figure 1. (a) Model of "kite" shape of **1** based on XRD data. In red: plane formed by the central phenyl ring. (b) Packing view of the **1** crystal.

[†] Aix Marseille Université.
[‡] University of Hull.
[§] Iwate University.

10.1021/ja807504k CCC: $40.75

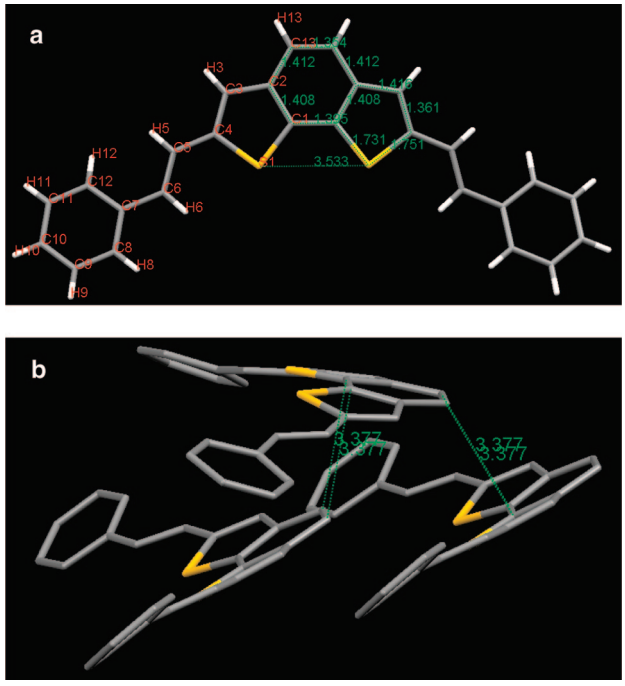

Figure 2. (a) Label atoms and bond length of **1**. (b) Close contacts between molecules of **1** with intermolecular C−C distances.

between sulfur atoms has an identical value (3.533 Å), but the bisthienobenzene core of **1** exhibits a curvature angle of 7.36° between the central phenyl and thiophene rings' planes. The main difference is the length of the bridge double bond, which decreases from 1.441 to 1.354 Å, indicative of a compression and a weakly aromatic character of the central plenyl ring of **1** (Figure 2a). In this context the only possibility for the fused core to maintain the S−S intramolecular interaction is to adopt a nonplanar geometry.

For the planes between thiophene rings and the double bond a 5.44° dihedral angle is measured. For **1** dihedral angles are observed on the same side of the central phenyl plane in a symmetrical twisted configuration of the fused bisthienobenzene core. This symmetrical twist is associated with a substantial degree of torsion of 12.01° between the central phenyl ring and the plane formed by the double bonds. Finally a rotational angle of 13.88° between the planes made up of the peripheral rings and the plane formed by thiophene ring, double bond, and C7, C10 is formed. Additionally the end-to-end molecular structure adopts a concave form. Therefore the overall molecular shape of **1** can be approximated by a "kite" shape or more precisely by that of a kitesurfing kite. **1** was found to crystallize in the orthorhombic space group *Pnam* with four equivalent molecules per unit cell.

The average molecular plane is perpendicular to the *ac*-plane. A quasi face-to-face packing with a tilt angle of 11.27° is measured between the average planes of the molecules, while for the related material **DS2T** a herringbone arrangement with an angle up to 60° was found.[8] Along the *a*-axis, molecules arrange in columns with an antiparallel orientation. Each molecule has 12 intermolecular contacts with 6 other molecules. In this structure **1** has four C−C intermolecular contacts with distances of 3.377 Å, clearly shorter than the sum of their van der Waals radii (C−C: 3.40 Å). The close $\pi-\pi$ stacking of **1** is due to the four C−C contacts between the fused central phenyl rings of one molecule with its two neighboring molecules (Figures 2b, S4−S8 and Table S1).

As expected for a rigid conjugated system UV−vis spectra of **1** in solution shows good resolution of the vibronic structure with maxima at 374, 393, and 416 nm (Figures S9).[10] A comparison

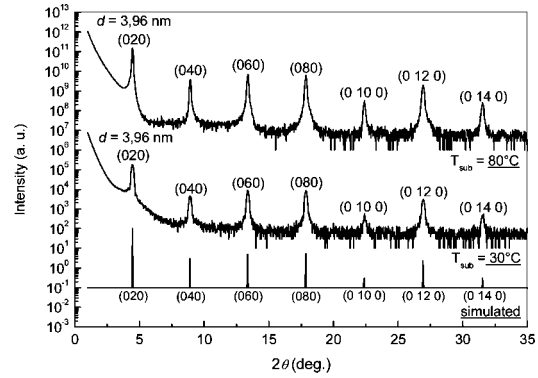

Figure 3. $\theta/2\theta$ mode of X-ray diffraction patterns of **1** thin film deposited at T_{sub} = 30 and 80 °C on Si/SiO_2 with a nominal thickness of 50 nm together with the simulated XRD peaks of **1** powder.

with **DS2T** reveals a hypsochromic shift of 32 nm for **1** indicating a reduction in the effective conjugation length attributing to the shape of the bisthienobenzene core that penalizes the delocalization of the π electrons which cannot form an extended conjugated pathway with both of its neighboring coupled styryl units. The chemical and thermal stability of **1** were investigated using UV−vis absorption spectroscopy and differential scanning calorimetry (DSC), and the results indicate that **1** can be heated repeatedly into the isotropic phase without any change of the crystallization behavior (Figures S10, S13).

$\theta/2\theta$ X-ray diffraction spectra of **1**-based thin films vacuum-deposited at 30 and 80 °C, with a nominal thickness of 50 nm, reveal that the films are characterized by sharp and strong reflections (Figure 3). The peaks can be indexed from the (020) to (0140) reflection, indicating that the *ac*-planes of the grains are oriented parallel to the substrate surface. Thin films consist of highly oriented polycrystals having an interplanar *d*(010)-spacing of 1.98 nm for both substrate temperatures. The value 1.98 nm corresponds to the molecular length determined by the single-crystal X-ray analysis, indicating nearly perfect orthogonal orientation of molecules onto the substrate. An interplanar *d*(020)-spacing of 3.96 nm corresponds to the *b*-axis in the unit cell (39.68 Å) which is just twice that of the monolayer thickness. Additionally, an exact agreement between simulated XRD peaks of **1** powder and maxima peaks observed in X-ray diffraction patterns of **1** thin films provides evidence that the molecular assembly in the thin film is the same as that in bulk crystal. Furthermore, similar XRD patterns of the thin film on substrate for both T_{sub} = 30 and 80 °C and for ultrathin films indicate that the crystalline phase was not affected by these parameters in the vacuum deposition (Figures S15−S16).

The thin-film morphology examined by AFM shows an apparent dependence on the substrate temperature. While a terrace-like step structure was observed for both T_{sub} values, small crystal grains ~1.5−3 μm in size were observed in the AFM images of thin films obtained at 30 °C (Figure 4a), and the grain size was increased at T_{sub} = 80 °C to ~3−7 μm as shown in Figure 4b and SEM pictures (Figures S17−S19).

1 shows well-defined linear and saturation-regime output characteristics (Figure 5a). The negative gate and source−drain voltages demonstrate that **1** is a p-channel material. The field effect mobilities calculated in the saturation regime were found to increase with substrate deposition temperature. This is due to an increased influence of the substrate temperature on the film morphology, where at higher temperatures better ordered thin films are formed. Furthermore, the hole mobility of OTFTs based on silicon oxide insulator layer coated with HDMS was significantly improved

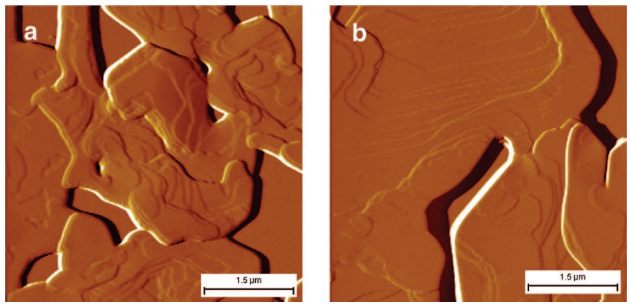

Figure 4. AFM pictures of **1** thin film deposited at T_{sub} = 30 °C (a) and 80 °C (b) on Si/SiO_2 with a nominal thickness of 50 nm.

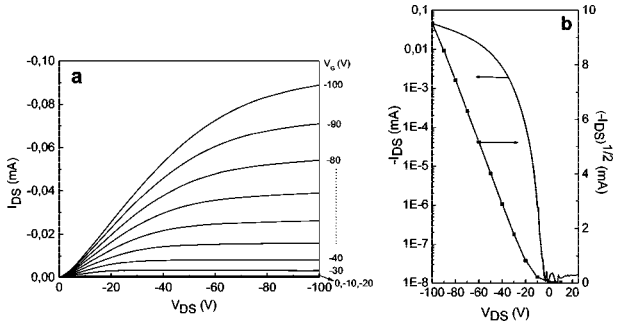

Figure 5. Output characteristic (a) and $I-V$ transfer plots (b) for **1** at T_{sub} = 80 °C on HMDS-SiO_2/Si.

Table 1. OTFT Data of the Semiconductors **1** Deposited at Different Substrate Temperatures on Bare SiO_2 or HMDS-SiO_2

T_{sub} (°C)	dielectric	μ (cm^2/V.s)	V_{th} (V)	I_{on}/I_{off}	S (V/decade)
30	bare SiO_2	$(1.4-1.7) \times 10^{-4}$	(−5)−(1.8)	(2−8) × 10^5	3−6
	HMDS-SiO_2	(1−8) × 10^{-3}	(−14)−(−15)	(1.8−2) × 10^5	4−6
80	bare SiO_2	0.005−0.02	(−5)−(12)	(0.5−3) × 10^5	4−5
	HMDS-SiO_2	0.08−0.1	(−12)−(−14)	(1.5−3) × 10^6	3−3.8

relative to the bare SiO_2 samples together with more negative threshold voltage ranges (Table 1). Hole mobilities as high as 0.1 cm^2/V.s for OTFT devices prepared at 80 °C on HMDS SiO_2 are achieved in the presence of air with a negative threshold voltage (V_{th}) of ∼ −14 V. Figure 5b shows the current−voltage transfer characteristics of a **1**-based OTFT device. OTFTs exhibit a very high I_{on}/I_{off} ratio (>10^6). The subthreshold swing (S), indicating how sharply the device turns on, is in the 3 V/decade range, and the turn-on voltage V_0 is −3 V.

In summary, a novel styryl end-capped benzo[2,1-*b*:3,4-*b*′]dithiophene semiconductor was synthesized and investigated. AFM imagery and XRD data reveal a preferential molecular orientation with the long axes along the substrate normal, where in-plane charge transport benefits from close $\pi-\pi$ stacking.

This has the surprising consequence that, although apparently being of a nonideal molecular shape, the molecular arrangement in **1**-based thin films is favorable for efficient charge transport across the SiO_2−semiconductor interface in an OTFT configuration. In particular, the reduced molecular conjugation length and the molecular shape are not limiting factors for the effective molecular overlap between adjacent molecules in the crystal structure. The highest mobility of **1** is 5 times higher than that of an unbridged counterpart. These results and structure property relationships point beyond this particular compound and highlight the need for a full correlation between molecular architecture and the assembly in the solid state to harness fully the potential of organic semiconductors.

Acknowledgment. The authors thank Prof. F. Fages from CINaM-UPR 3118 for his critical reading and the "Agence Nationale de la Recherche" for supporting this work (Grant ANR-06-BLAN-0295).

Supporting Information Available: Synthetic procedures for **1**−**4** with NMR; X-ray crystallographic analysis of **DS2T** and **1**; UV−vis data; cyclic voltammetry; DSC characterizations; DFT calculations; device fabrications; XRD; AFM and MEB pictures of thin films. This material is available free of charge via the Internet at http://pubs.acs.org.

References

(1) Murphy, A. R.; Fréchet, J. M. J. *Chem. Rev.* **2007**, *107*, 1066.
(2) Anthony, J. E. *Chem. Rev.* **2006**, *106*, 5028.
(3) Pascal, R. A., Jr. *Chem. Rev.* **2006**, *106*, 4809.
(4) (a) Laquindanum, J. G.; Katz, H. E.; Lovinger, A. J.; Dodabalapur, A. *Adv. Mater.* **1997**, *9*, 36. (b) Li, X. C.; Sirringhaus, H.; Garnier, F.; Holmes, A. B.; Moratti, S. C.; Feeder, N.; Clegg, W.; Teat, T. S.; Friend, R. H. *J. Am. Chem. Soc.* **1998**, *120*, 2206. (c) Sirringhaus, H.; Friend, R. H.; Wang, C.; Leuninger, J.; Mullen, K. *J. Mater. Chem.* **1999**, *9*, 2095. (d) Sirringhaus, H.; Friend, R. H.; Li, X. C.; Moratti, S. C.; Holmes, A. B.; Feeder, N. *Appl. Phys. Lett.* **1997**, *71*, 3871. (e) Iosip, M. D.; Destri, S.; Pasini, M.; Porzio, W.; Pernstich, K. P.; Batlogg, B. *Synth. Met.* **2004**, *146*, 251. (f) Zhang, X.; Matzger, A. J. *J. Org. Chem.* **2003**, *68*, 9813. (g) Zhang, X.; Cote, A. P.; Matzger, A. J. *J. Am. Chem. Soc.* **2005**, *127*, 10502. (h) Xiao, K.; Liu, Y.; Qi, T.; Zhang, W.; Wang, F.; Gao, J.; Qiu, W.; Ma, Y.; Cui, G.; Chen, S.; Zhan, X.; Yu, G.; Qin, J.; Hu, W.; Zhu, D. *J. Am. Chem. Soc.* **2005**, *127*, 13281. (i) Nenajdenko, V. G.; Sumerin, V. V.; Chernichenko, K. Y.; Balenkova, E. S. *Org. Lett.* **2004**, *6*, 3437. (j) Noh, Y. Y.; Azumi, R.; Goto, M.; Jung, B. J.; Lim, E.; Shim, H. K.; Yoshida, Y.; Yase, K.; Kim, D. Y. *Chem. Mater.* **2005**, *17*, 3861. (k) Ando, S.; Nishida, J. I.; Fujiwara, E.; Tada, H.; Inoue, Y.; Tokito, S.; Yamashita, Y. *Chem. Mater.* **2005**, *17*, 1261. (l) Meng, H.; Sun, F.; Goldfinger, M. B.; Jaycox, G. D.; Li, Z.; Marshall, W. J.; Blackman, G. S. *J. Am. Chem. Soc.* **2005**, *127*, 2406. (m) Merlo, J. A.; Newman, C. R.; Gerlach, C. P.; Kelley, T. W.; Muyres, D. V.; Fritz, S. E.; Toney, M. F.; Frisbie, C. D. *J. Am. Chem. Soc.* **2005**, *127*, 3997. (n) Deman, A. L.; Tardy, J.; Nicolas, Y.; Blanchard, P.; Roncali, J. *Synth. Met.* **2004**, *146*, 365. (o) Nicolas, Y.; Blanchard, P.; Roncali, J.; Allain, M.; Mercier, N.; Deman, A. L.; Tardy, J. *Org. Lett.* **2005**, *7*, 3513. (p) Takimiya, K.; Kunugi, Y.; Toyoshima, Y.; Otsubo, T. *J. Am. Chem. Soc.* **2005**, *127*, 3605.
(5) (a) Curtis, M. D.; Cao, J.; Kampf, J. W. *J. Am. Chem. Soc.* **2004**, *126*, 4318. (b) da Silva Filho, D. A.; Kim, E.-G.; Brédas, J.-L. *Adv. Mater.* **2005**, *17*, 1072.
(6) (a) Videlot-Ackermann, C.; Ackermann, J.; Brisset, H.; Kawamura, K.; Yoshimoto, N.; Raynal, P.; El Kassmi, A.; Fages, F. *J. Am. Chem. Soc.* **2005**, *127*, 16346. (b) Videlot-Ackermann, C.; Ackermann, J.; Kawamura, K.; Yoshimoto, N.; Brisset, H.; Raynal, P.; El Kassmi, A.; Fages, F. *Org. Electronics* **2006**, *7*, 465.
(7) Kawase, T.; Kurata, H. *Chem. Rev.* **2006**, *106*, 5250.
(8) Crystal data for **1** (CCDC 695940) and **DS2T** (CCDC 693725) contain the supplementary crystallographic data for this paper. These data can be obtained free of charge from The Cambridge Crystallographic Data Centre via www.ccdc.cam.ac.uk/data_request/cif.
(9) Brusso, J. L.; Hirst, O. D.; Dadvand, A.; Ganesan, S.; Cicoira, F.; Robertson, C. M.; Oakley, R. T.; Rosei, F.; Perepichka, D. F. *Chem. Mater.* **2008**, *20* (7), 2484.
(10) Jaffé, H. H.; Orchin, M. *Theory and Applications of Ultraviolet spectroscopy*; Wiley: New York, 1962.

JA807504K